Structural properties of the human respiratory syncytial virus P protein: Evidence for an elongated homotetrameric molecule that is the smallest orthologue within the family of paramyxovirus polymerase cofactors

María T. Llorente,[1,2] Ian A. Taylor,[3] Eduardo López-Viñas,[4,5] Paulino Gomez-Puertas,[4,5] Lesley J. Calder,[3] Blanca García-Barreno,[1,2] and José A. Melero[1,2]*

[1] Centro Nacional de Microbiología, Instituto de Salud Carlos III, Majadahonda, 28220 Madrid, Spain

[2] CIBER de Enfermedades Respiratorias, Instituto de Salud Carlos III, Majadahonda, 28220 Madrid, Spain

[3] National Institute for Medical Research, The Ridgeway, Mill Hill, London NW7 1AA, United Kingdom

[4] Centro de Biología Molecular "Severo Ochoa" (CSIC-UAM), Cantoblanco, 28049 Madrid, Spain

[5] CIBER-Obn Physiopathology of Obesity and Nutrition (CB06/03/0026), Instituto de Salud Carlos III, Spain

ABSTRACT

The oligomeric state and the hydrodynamic properties of human respiratory syncytial virus (HRSV) phosphoprotein (P), a known cofactor of the viral RNA-dependent RNA polymerase (L), and a trypsin-resistant fragment (X) that includes its oligomerization domain were analyzed by sedimentation equilibrium and velocity using analytical ultracentrifugation. The results obtained demonstrate that both P and fragment X are homotetrameric with elongated shapes, consistent with electron micrographs of the purified P protein in which thin rod-like molecules of ~12.5 ± 1.0 nm in length were observed. A new chymotrypsin resistant fragment (Y) included in fragment X has been identified and purified by gel filtration chromatography. Fragment Y* may represent a minimal version of the P oligomerization domain. Thermal denaturation curves based on circular dichroism data of P protein showed a complex behavior. In contrast, melting data generated for fragments X and particularly fragment Y* showed more homogeneous transitions indicative of simpler structures. A three-dimensional model of X and Y* fragments was built based on the atomic structure of the P oligomerization domain of the related Sendai virus, which is in good agreement with the experimental data. This model will be an useful tool to make rational mutations and test the role of specific amino acids in the oligomerization and functional properties of the HRSV P protein.*

Proteins 2008; 72:946–958.
© 2008 Wiley-Liss, Inc.

Key words: respiratory syncytial virus; phosphoprotein hydrodynamics and oligomerization; thermal denaturation; 3-D modeling; paramyxovirus polymerase cofactors.

INTRODUCTION

Human respiratory syncytial virus (HRSV) is the prototype of the genus *Pneumovirus* of the *Paramyxoviridae* family. The genome of HRSV is a nonsegmented single-stranded RNA molecule of negative polarity, comprising 15,222 nucleotides for the A2 strain.[1] HRSV has 10 genes, arranged linearly along the genome, that encode 11 different proteins.[2,3] Replication and transcription of the HRSV genome conforms to the general pattern observed in other paramyxoviruses; that is, the viral genes are transcribed sequentially from a single 3′ end promoter, and replication involves the synthesis of a positive-sense antigenome that is an exact complement of the genome.

The template for replication and transcription is the HRSV ribonucleoprotein (RNP) complex, made of the genome (or the antigenome) and the nucleoprotein (N) that covers the entire RNA length and protects it from RNase attack. RNA synthesis is catalyzed by the RNA-dependent RNA polymerase, encoded by the L gene.[4] Genome replication and transcription requires the viral phosphoprotein (P) as an essential cofactor of the viral polymerase. In addition, efficient transcription also requires the first product of the M2 gene (the M2-1 or 22k protein) as an antitermination

factor of the polymerase.[5] While P proteins are encoded by all paramyxoviruses, 22k is unique to members of the *Pneumovirinae* subfamily (including HRSV) of the *Paramyxoviridae* family.[6]

HRSV P (241 amino acids) is the shortest phosphoprotein encoded by all paramyxoviruses, and therefore provides a useful structural archetype of this type of protein, since it is apparent that all paramyxovirus Ps have similar functions in the replication and transcription of their respective templates. It has been postulated from studies originating from Sendai virus, that P has a dual role in genome replication and transcription. On the one hand P, through amino acids located near its N-terminus, acts as a chaperone of newly synthesized N (N^0) to prevent its illegitimate assembly and facilitate its delivery to the nascent RNA chain during genome replication.[7,8] On the other hand, P cartwheels on the template by simultaneous breaking and reforming of contacts between a C-terminal segment of P and the protomeric N of the RNP complex, opening this structure so that the polymerase tethered by P can access the bases in the viral RNA.[9–12] HRSV P seems to follow this general model as it has been shown that the C-terminal end of this molecule interacts with N-RNA[13–15] and that, in addition, P interacts with the RNA-dependent RNA polymerase[16] and possibly with the 22k protein,[17] playing a central role in all processes of RNA synthesis.

The oligomeric nature of the paramyxovirus P protein is central to its function. Thus, while monomeric Sendai virus P can still bind to RNPs, this interaction is nonfunctional for viral RNA synthesis,[10] probably because simultaneous binding of several P monomers to assembled N protomers is required by P to move along the RNP template. The atomic structure of the Sendai virus P oligomerization domain has been solved by X-ray crystallography and shown to be a homotetrameric coiled-coil.[18] Similarly, structural data of the rinderpest virus P protein indicate that it is also homotetrameric.[19] However, there is some controversy about the oligomeric status of the HRSV P protein. Originally, it was proposed that HRSV P was a homotetramer, based on crosslinking studies with bifunctional reagents.[14,20] Subsequently, conflicting results have been reported with regard to the behavior of P in gel filtration chromatography[14,20,21] including one report, where homodimerization of HRSV P has been proposed.[22]

In a previous study, a trypsin-resistant fragment of HRSV P (fragment X) was identified and partially characterized.[21] Fragment X, which eluted as an anomalously high molecular weight species from a gel filtration column, was shown to be oligomeric and to have a high α-helical content. These characteristics resemble those of the oligomerization domains of other paramyxoviruses[18,19,23] and indicate that fragment X was, or included, the oligomerization domain of HRSV P. To clarify the oligomeric status of HRSV P and to gain insights into its three-dimensional structure, we have carried out sedimentation equilibrium and velocity analysis of purified HRSV P and fragment X. In addition, thermostability studies of HRSV P, fragment X and a newly identified chymotrypsin-resistant fragment Y*, included in fragment X, have provided information about the structural complexity of HRSV P and its oligomerization domain. Finally, a model of the HRSV P oligomerization domain was built using homology modeling procedures that is in good agreement with the experimental data and that may help to direct future mutagenic studies designed to relate structure to function in this important HRSV polymerase cofactor.

MATERIALS AND METHODS

Purification of HRSV P protein and protease-resistant fragments

Production and purification of HRSV P protein and the trypsin-resistant fragment X have been reported.[21] Briefly, HEp2 cells were infected with a recombinant vaccinia virus that encodes HRSV P. Extracts were made and the P protein was purified by immunoaffinity chromatography using a previously described monoclonal antibody (1P) that recognizes an epitope near the N-terminal end of HRSV P.[24] The protein eluted from the antibody column was further purified by gel filtration chromatography using a Superdex 200 HR 10/30 column. The purified P protein was digested with proteomic grade recombinant trypsin (Roche) for 1 h at 37°C at a ratio of 5:1 (protein:trypsin, w/w). The digestion products were separated by gel filtration and elution of the trypsin-resistant fragment X was monitored by Western blotting of column fractions with the monoclonal antibody 021/2P.[21]

Fragment Y was generated by digestion of purified HRSV P with a mixture of trypsin and sequencing grade chymotrypsin (Roche) at a ratio of 5:1:0.1 (protein:trypsin:chymotrypsin, w/w) for 1 h at 37°C. Digestion products were separated by gel filtration chromatography, and elution of fragment Y was monitored by SDS-PAGE and Coomassie blue staining of fraction samples.

Analytical ultracentrifugation

Sedimentation equilibrium

Sedimentation equilibrium experiments were performed at 293 K in a Beckman Optima XLA analytical ultracentrifuge using six-channel centrepieces in an An-60 Ti rotor. Prior to centrifugation, samples were dialysed exhaustively against the buffer blank, 10 mM Tris-HCl, pH 7.5, 150 mM NaCl. After centrifugation for 18 h, radial scans of the cells were performed at 2-h intervals ($\lambda = 230$ nm). Scans were overlaid to determine whether the absorbance profile was static and that equilibrium had been established, and then the rotor speed was

increased and the procedure repeated. Data were collected on three samples of P and fragment X, at concentrations ranging from 0.15 to 0.25 mg/mL, and three rotor speeds: 8000, 12,000, and 16,000 rpm for P and at 17,000, 20,000, and 23,000 rpm for fragment X. Protein partial specific volumes and the solvent density were calculated from tabulated values.[25] The program SED-PHAT[26,27] was used to determine weight-averaged molecular weights by nonlinear fitting of individual equilibrium profiles (A vs. r) to a single-species ideal solution model. Inspection of these data revealed that the molecular weights showed no concentration dependency, and so global fitting incorporating the data from multiple speeds and sample concentrations was applied to extract the final molecular weight.

Sedimentation velocity

Sedimentation velocity experiments were performed in a Beckman Optima XLA analytical ultracentrifuge, using conventional aluminium double-sector quartz cells in an An-60 Ti rotor. Rotor speeds were 40,000 and 58,000 rpm for P and fragment X, respectively, and the temperature was maintained at 293 K. Prior to centrifugation, protein samples were dialysed exhaustively against the buffer blank, 10 mM Tris-HCl pH 7.5, 150 mM NaCl. The protein concentration was 0.35 mg/mL, and during experiments, radial scans were collected every 300 s at $\lambda = 230$ nm for 500 min. The data recorded from moving boundaries were analyzed in terms of both discrete species and continuous size distribution functions of sedimentation coefficient, $C(S)$ and molar mass, $C(M)$ using the program SEDFIT.[26,28]

Electron microscopy

Protein samples in buffer 10 mM Tris-HCl (pH 7.5) and 150 mM NaCl were absorbed onto carbon films and stained with 1% sodium silicotungstate (pH 7.0). A JEOL 1200 electron microscope, operated at 100 kV, was used to view the samples. Micrographs were taken under minimum-dose, accurate defocus conditions to preserve details to $\approx$1.5 nm.[29]

Circular dichroism

Samples in 0.01M phosphate buffer (pH 7.0) at a concentration of ~0.2 mg/mL, determined by $OD_{280 \text{ nm}}$, were analyzed in a JASCO 810 spectropolarimeter at room temperature with a 1 mm cell. Ten spectra were recorded between 190 and 260 nm and averaged. The scan rate was 50 nm/min with a delay time of 60 s. Spectra of buffer alone were recorded and subtracted from protein spectra. Molar residue ellipticity (MRE) values were calculated using the spectra analysis of the Jasco Spectra Management software. The α-helix content was calculated as described.[30]

For thermal denaturation studies, samples at a concentration of ~0.2 mg/mL were heated stepwise as indicated in the figure legends. The temperature between steps was increased at a rate of 2°C/min. At each step, five spectra were recorded (190–260 nm) at a scanning speed of 50 nm/min and a delay time of 180 s, and averaged. After reaching the highest temperature (90–95°C as indicated in the figure legends), samples were cooled stepwise and spectra recorded as indicated for heating. Raw data were converted to MRE, and the $MRE_{222 \text{ nm}}$ values were plotted for each temperature to generate the thermal denaturation/renaturation curves of each sample.

Mass spectrometry

Samples were mixed with an aliquot of α-cyano-4-hydroxycinnamic acid (Bruder Daltonics) in 50% aqueous acetonitrile and 0.15% trifluoroacetic acid. This mixture was deposited onto the matrix-assisted laser desorption ionization (MALDI) probe and allowed to dry at room temperature. MALDI spectra were measured as previously described.[21]

Model building

Sequences similar to HRSV P protein were obtained from the databases using Blast[31] and aligned using ClustalW algorithm.[32] The structural model of the tetramerization domain of HRSV P was built using homology modeling procedures, based on multiple sequence alignment of paramyxovirus P proteins and the crystallographic coordinates of the multimerization domain of Sendai virus P[18] (Protein Data Bank (PDB) entry: 1EZJ). The three-dimensional model was built using the SWISS-MODEL server facilities (http://www.expasy.ch/swissmod/SWISS-MODEL.html).[33–35] Its structural quality was checked using the WHAT-CHECK routines[36] from the WHAT IF program[37] from the same server. Finally, to optimize geometry, release local constraints, and correct possible bad contacts, the modeled structure was energy minimized with the implementation of the GROMOS 43B1 force field of the program DeepView,[33] using 500 steps of steepest descent minimization followed by 500 steps of conjugate-gradient minimization. Protein structures, atomic surfaces, and electrostatic potentials representation were generated using Pymol (W.L. DeLano, 2002, DeLano Scientific, San Carlos, CA).

RESULTS

Oligomeric and hydrodynamic properties of the HRSV P protein and the trypsin-resistant fragment X

Purification of both the HRSV P protein and the trypsin-resistant fragment X have been reported previ-
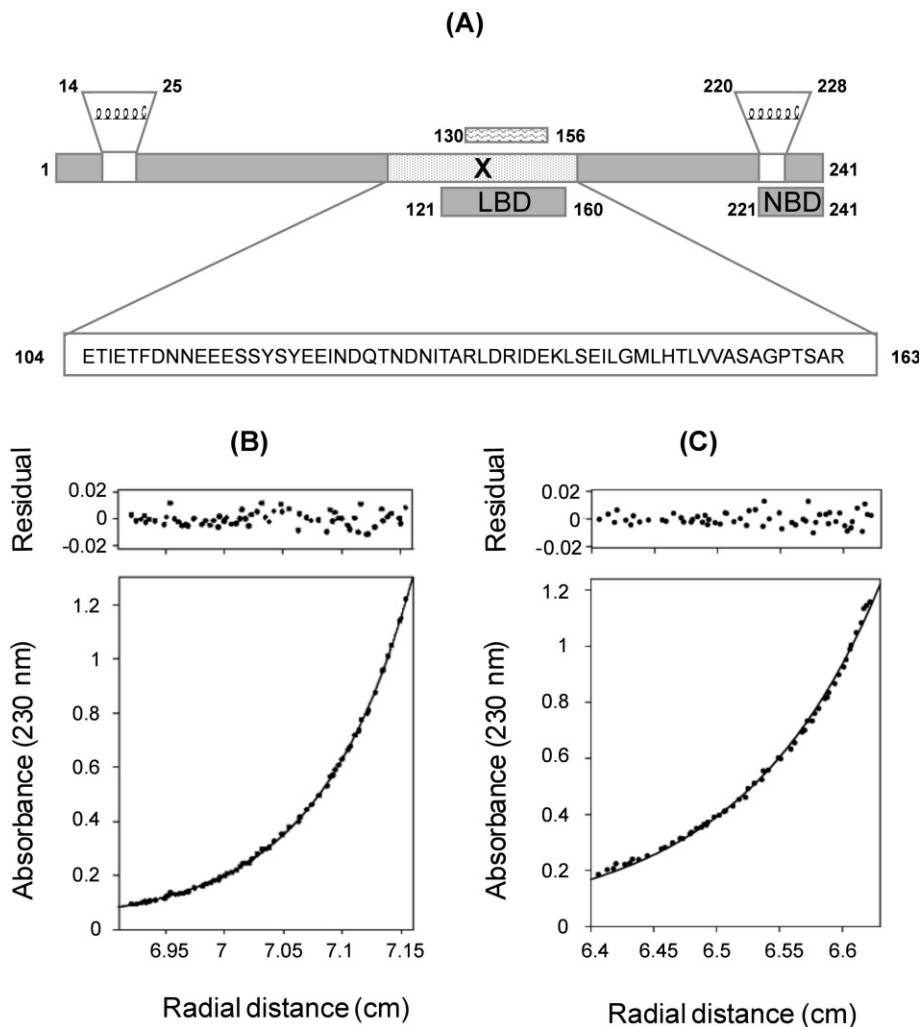
(A)

(B)   **(C)**

<div style="background-color:#dce6f0; padding:10px;">

Figure 1

*Equilibrium sedimentation of HRSV P and fragment X. A diagram of the HRSV P protein primary structure is represented (**A**), indicating the location (aa 104–163) and amino acid sequence of fragment X, the location of the L-polymerase-binding domain[16] (LBD), and the N-binding domain[13] (NBD). Two predicted α-helices within the N- (aa 14–25) and C- (220–228) terminal ends, and a region (aa 130–156) that displays a distribution of hydrophobic clusters that typifies coiled coils are indicated.[21] Both P (**B**) and fragment X (**C**), purified as indicated under Materials and Methods, were used in equilibrium sedimentation experiments. Data are presented as circles and the fitted curves by lines. These plots correspond to the equilibrium distributions produced from an initial concentration of 0.2 mg/mL at a rotor speed of 12,000 rpm for P protein and 0.2 mg/mL at a rotor speed of 20,000 rpm for fragment X. The residuals of the fitted data are shown above each panel.*

</div>

ously.[21] Figure 1(A) shows a diagram of the P protein primary structure, indicating predicted structural elements and the location and amino acid sequence of fragment X. To assess their oligomeric status, both P and fragment X were analyzed by sedimentation equilibrium, employing multiple speeds and protein concentrations. Figure 1(B,C) shows representative results of such experiments for P and fragment X, respectively. The average molecular masses derived under these experimental conditions were 100 ± 9 kDa and 27 ± 2.5 kDa, and the global values obtained for the best fit of all experimental data were 104.6 and 28.3 kDa for P and fragment X, respectively (Table I). No trend of increasing molecular weight with increasing protein concentration over the range the experiments were conducted was apparent. Moreover, the low values of local root-mean-square deviation (RMSD) and global reduced χ^2, together with the small magnitude and random distribution of residuals [top panels, Fig. 1(B,C)], indicate that the fits were of good quality. On the basis of these observations and the fact that the molecular weights we have determined are in good agreement with the theoretical molecular masses of tetramers of both P protein (108,592 Da) and fragment X (26,988 Da) molecules, respectively, our interpretation is that P undergoes self-association into a tetramer that is stable at the protein

Table I

Hydrodynamic Parameters of P and Fragment X

| Parameter	P protein	Fragment X
M_r (kDa)	27,148	6,747
$\overline{V}$	0.721	0.714
M_w (SE) Av (kDa)	100 ± 9	27 ± 2.5
M_w (SE) Global (kDa)	104.6	28.3
Average local RMSD (global fit)	0.005	0.008
Global reduced χ^2	1.35	2.70
$S_{20,w}$	3.72 ± 0.02	2.21 ± 0.01
$D_{t,20,w}$	3.6 ± 0.1	6.46 ± 0.1
f/f_0	2.28 ± 0.1	1.56 ± 0.1

M_r, molecular weight estimated from amino acid sequences; $\overline{V}$, partial specific volume; M_w Av, average of the molecular weight and standard deviations estimated by sedimentation equilibrium (SE) at three different speeds and three protein concentrations; M_w Global, molecular weight obtained from global fit of the whole data set from SE experiments; RMSD, average local root mean square deviation; $S_{20,w}$, sedimentation coefficient obtained by velocity sedimentation (SV); $D_{t,20,w}$, translational diffusion coefficient; f/f_0, frictional ratio derived from data.

concentrations used in our analysis. This autoassembly of P into tetramers should not involve formation of disulfide bonds, since P has no cysteines.

Sedimentation velocity experiments (Fig. 2) demonstrated that P and fragment X preparations contain only a single component. Data from both P and X experiments fit well to a single discrete species model, with $S_{20,w}$ values of 3.72 ± 0.02 and 2.21 ± 0.01, respectively (Table I). Moreover, inspection of the respective $C(S)$ functions reveals that they contain a major peak comprising >97% of the loading signal (Fig. 2). In both, P and X experiments, the peak is centered at the $S_{20,w}$ obtained from the discrete component analysis. In both samples, this major peak is accompanied by a minor peak that contributes less than 3% of the loading signal. The minor peak has $S_{20,w}$ of 5.9 in the P sample and 3.8 in the X sample with corresponding M_w of 200 kDa and 56 kDa, respectively. Whether this small amount of material constitutes an octomeric higher order assembly of P and X or a minor contaminant of the protein preparations is still unclear. The presence of these minor peaks will bias the weight-averaged molecular weights, determined from the sedimentation equilibrium data, but only by around 5%. Nevertheless, $C(M)$ analysis of data yielded molecular masses of 98 kDa and 30 kDa for the major peaks in
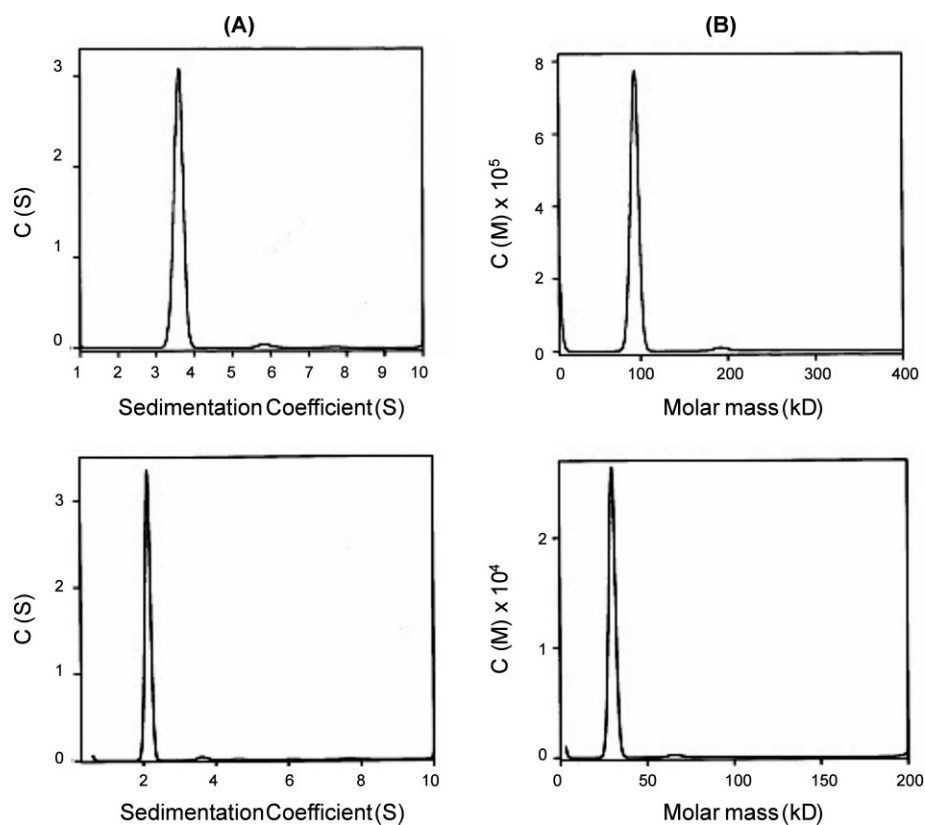
Figure 2

*Velocity sedimentation measurements of P and fragment X. Best fit C(S) (**A**) and C(M) (**B**) functions for P (upper panels) and fragment X (lower panels) obtained from sedimentation velocity experiments, at a concentration of 0.35 mg/mL and speeds of 40,000 rpm and 58,000 rpm for P and fragment X, respectively (see Materials and Methods).*
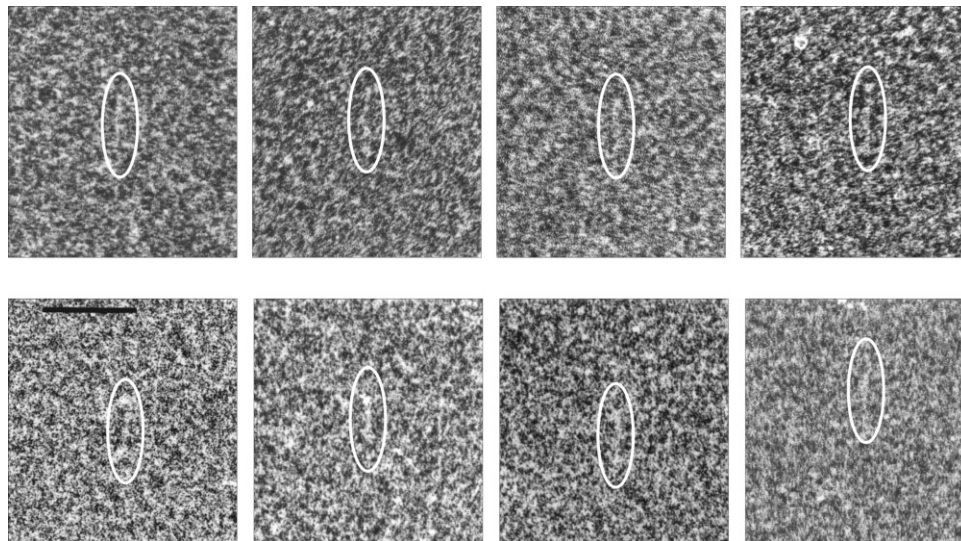
Figure 3

Electron microscopy of HRSV P protein. Gallery of negatively stained P protein molecules, enclosed in ellipses, observed under the electron microscope (see Materials and Methods). Bar, 20 nm.

the P and fragment X preparations, respectively, that are in good agreement with the molecular masses determined by the discrete component analysis and by sedimentation equilibrium of the respective molecules (Table I). These data allowed us to calculate other hydrodynamic parameters for P and fragment X, including their frictional ratio (f/f_0) a measure of the degree of asymmetry in a molecule with respect to a sphere of the same mass (Table I). The f/f_0 ratios derived for tetramers of P and X deviate considerably from 1.00, the value that would be obtained if the molecules were anhydrous and spherical, and so even accounting for a degree of hydration, these results demonstrate that fragment X and particularly HRSV P protein have very elongated shapes.

In order to obtain independent information about the shape of HRSV P, visualization of negatively stained purified P protein was attempted by electron microscopy (Fig. 3). Despite the limitations of this technique for observation of small size molecules, thin rod-like molecules of ~12.5 ± 1.0 nm in length were observed only in grids prepared with the purified P protein. The uniform length of these molecules provided convincing evidence that the rods, distinctive above the grainy background of the stain, represented the P molecules. Their elongated shape is consistent with the f/f_0 ratio calculated for the P protein that gave dimensions in 100-Å range for the long axis when the protein is modeled as either a prolate ellipsoid or a rod (not shown).

In summary, the sedimentation behavior of the P protein indicates that it is a homotetrameric molecule with an elongated shape, consistent with the shape of molecules observed by electron microscopy. The hydrodynamic parameters of fragment X are in agreement with the previous assumption that this trypsin-resistant fragment is also tetrameric and that it has an elongated shape, probably a consequence of its high α-helical content.[21]

Thermal denaturation of P and fragment X

To assess the thermal stability of HRSV P and fragment X, far UV circular dichroism (CD) spectra of both molecules were recorded as a function of temperature. Plots of the MRE at 222 nm ($MRE_{222\ nm}$), indicative of the α-helical content, against temperature for P and fragment X are shown in Figure 4(A,B).

P protein showed a continuous and gradual reduction in intensity of $MRE_{222\ nm}$ when the sample temperature was raised from 20 to 90°C without a precise transition at any temperature [Fig. 4(A)]. Stepwise cooling of the P protein sample resulted in some recovery of the CD intensity of $MRE_{222\ nm}$, but it did not return to the original value. These results are interpreted as indicative that the P protein contains multiple structural elements that, although they contribute to the overall CD at 222 nm, melt at different temperatures and have different degrees of reversibility.

The denaturation curve of fragment X was significantly different from that of the P protein. A gradual loss in the intensity of MRE at 222 nm was observed when fragment X was heated from 20°C up to ~75°C. This was followed by a steep transition above 75°C. Cooling of fragment X
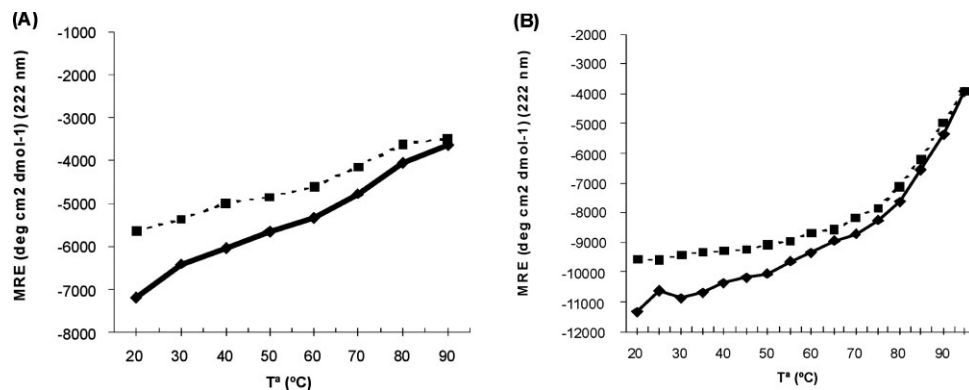
Figure 4

*Thermostability of HRSV P and fragment X. Purified P protein (**A**) and fragment X (**B**) were heated stepwise (continuous line) from 20 up to 90°C or from 20 up to 95°C. At intervals of 10°C or 5°C, respectively, five CD spectra (190–260 nm) were recorded, and the MRE values at 222 nm, derived from the average spectra, were calculated. After reaching the highest temperature, samples were cooled down stepwise (broken line) at intervals of 10°C and 5°C for protein P and fragment X, respectively. CD spectra were recorded and the ellipticity values at 222 nm plotted at the different temperatures.*

led to an increase in the intensity of MRE at 222 nm that reversed the heat-denaturation curve down to 70°C and that leveled off below this temperature. These results provide evidence that fragment X contains at least two structural motifs, one melting largely uncooperatively between 20 and 75°C, and the other showing cooperative and reversible transition above 75°C.

Isolation and characterization of a subsegment of fragment X resistant to chymotrypsin

Since the thermal denaturation curve indicated that fragment X [Fig. 4(B)] might contain more than one structural motif, further limited proteolytic digestion was undertaken in order to subdivide fragment X into individual structural elements.

In a previous study,[21] digestion of P with TPCK-trypsin yielded a major product that was identified as fragment X by N-terminal sequencing and mass spectrometry; however, a minor product of lower molecular mass was found in some preparations. This minor product was a subfragment of X, and may have been generated by chymotrypsin activity contaminating the TPCK-trypsin used in those studies. Therefore, P protein was doubly digested with a mixture of sequencing grade trypsin and chymotrypsin. This was followed by gel filtration chromatography, as described previously for fragment X. A peak eluting as a ~120 kDa species showed a single band of ~9 kDa in a SDS-PAGE gel [labeled Y* in Fig. 5(B)], that migrated faster than fragment X.

Homogeneity of the preparations of fragment X and the newly identified fragment Y* was checked by mass spectrometry. Fragment X [Fig. 5(C)] contained a major

species of 6748.9 Da that fits well with its theoretical mass of 6748 Da, calculated from the reported sequence[21] and a minor subspecies of 6829.3 Da that was identified as an adduct of phosphorylated X at Ser 119 (not shown).

N-terminal sequencing of fragment Y* yielded a single sequence (N-SYEEINDQ) starting at Ser 119 (not shown). The mass spectrum of fragment Y* [Fig. 5(D)] contained a major species of 4645.4 Da that fits well with the mass of a P fragment starting at Ser 119 and ending at Thr160 [Fig. 5(A)]. Therefore, fragment Y* is three amino acid shorter at the C-terminus than the previously described minor subproduct of fragment X.[21] The mass spectrum of fragment Y* had also a minor phosphorylated adduct of 4724.7 Da and, in addition, a very minor peak of 4394.5 Da that is consistent with a shortened fragment Y* lacking the first two N-terminal amino acids. In any case, the results of Figure 5(C,D) indicate a high degree of homogeneity of the preparations of fragment X and Y* used in this study. It is also noticeable that the migration of P and fragments X and Y* in SDS-PAGE gels [Fig. 5(B)] is substantially slower than expected from their respective masses.
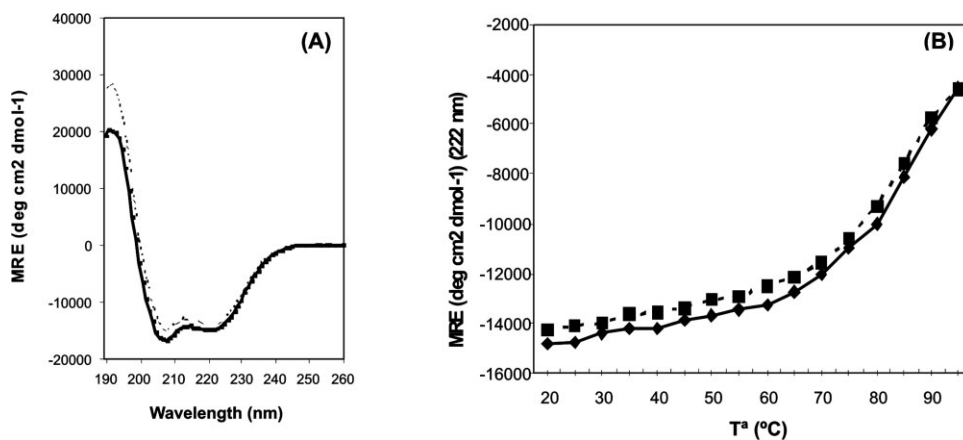
The far-UV CD spectrum of fragment Y* was very similar to that of fragment X indicative of a high α-helical content [Fig. 6(A)]. To test whether fragment Y* may contain some of the substructures inferred from the thermal denaturation curves of fragment X, purified fragment Y* was heated stepwise from 20°C up to 95°C and its CD spectra recorded at different temperatures [Fig. 6(B)]. The plot of MRE$_{222\ nm}$ against temperature revealed a melting profile with a steep transition between 70 and 95°C (midpoint at ~85°C), indicating that fragment Y* contains apparently a homogeneous structural motif with a high
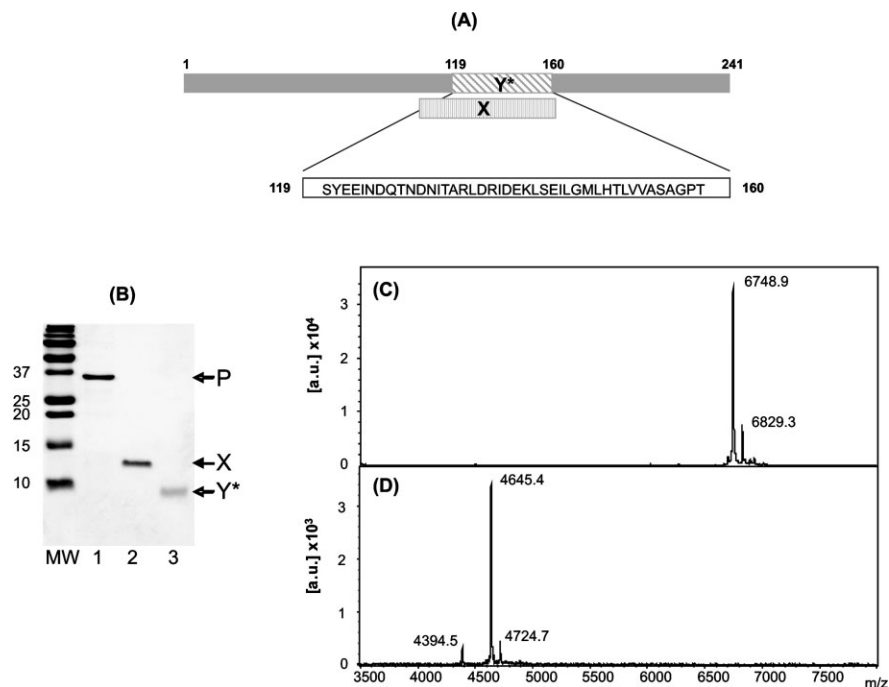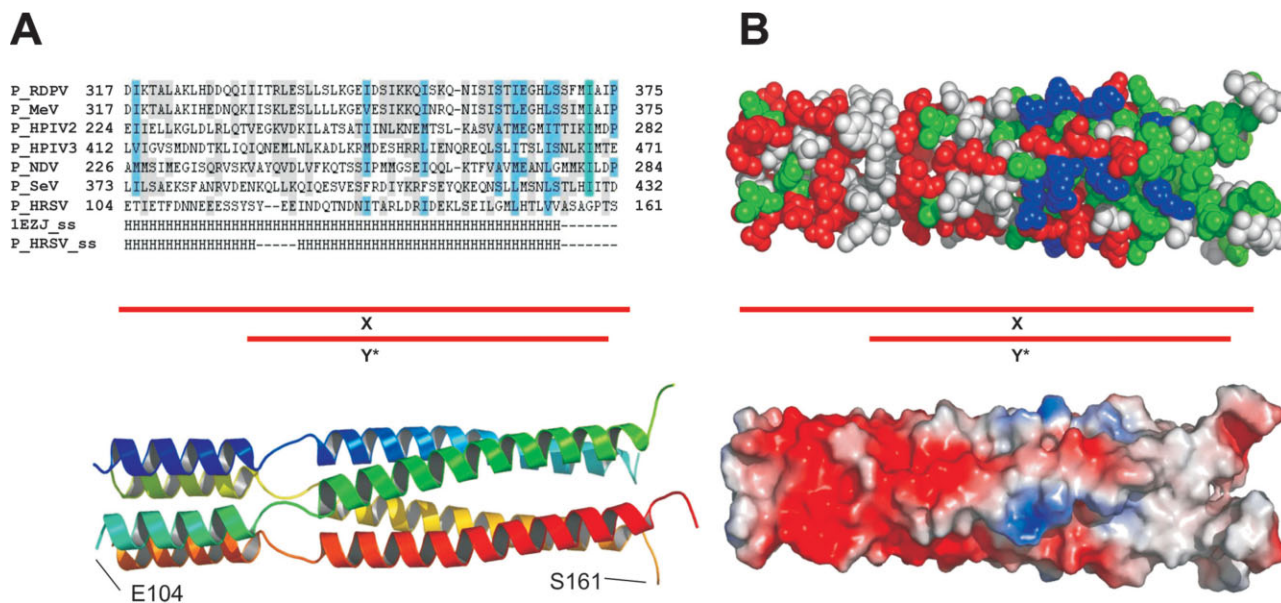
Figure 5

Characterization of fragment Y*. (**A**) Localization of the previously described fragment X[21] and the newly identified fragment Y*, whose amino acid sequence is indicated, in the P protein primary structure. (**B**) P, X, and Y* (lanes 1, 2, and 3, respectively) purified by gel filtration chromatography were analyzed by SDS-PAGE and Coomassie stained; MW, molecular weight standards. Mass spectra of purified fragments X (**C**) and Y* (**D**) recorded in a linear mode.

α-helical content. After stepwise cooling of fragment Y* from 95°C down to 20°C, an almost complete gain of MRE at 222 nm was observed. Thus, fragment Y* apparently represents a homogenous α-helical structural element, which experiences an almost reversible denaturation/renaturation transition after a single cycle of heating and cooling, and that may correspond to the minimal oligomerization domain of the native HRSV P protein.

Figure 6

CD and thermostability of fragment Y*. (**A**) Far-UV CD spectrum of fragment Y* (broken line) compared to that of fragment X (solid line) at 20°C. (**B**) Fragment Y* was heated from 20 up to 95°C (continuous line), cooled down to 20°C (broken line) and spectra were recorded at 5°C intervals as indicated in Figure 4.

Figure 7

3D model of the HRSV phosphoprotein oligomerization domain. (**A**) Top panel: Structure-based multiple alignment of partial P sequences from representative viruses belonging to the Paramyxoviridae family (P_RDPV: rinderpest virus; P_MeV: measles virus; P_HPIV _2 and _3: human parainfluenza virus 2 and 3, respectively; P_NDV: Newcastle disease virus; P_SeV: Sendai virus; P_HRSV: human respiratory syncytial virus). Residues are colored according to conservation. Helical elements (H) of the multimerization domain of Sendai virus phosphoprotein (1EZJ_ss), present in the crystallized structure, are shown, as well as predicted location of α-helices in the structural model of the HRSV P oligomerization domain (P_HRSV_ss). The position of X and Y fragments in HRSV P protein sequence is indicated (red bars). Bottom panel: Ribbon-based 3-D modeled structure of the HRSV P oligomerization domain (residues 104–161), based on the crystallographic coordinates of the SeV P protein multimerization domain (PDB: 1EZJ) and the multiple sequence alignment for P proteins of the Paramyxoviridae family. (**B**) Top panel: atomic volume representation of residues in HRSV P fragment X, colored according to their physicochemical properties: white, polar and noncharged; red, negative; blue, positive; green, hydrophobic. Most hydrophobic residues were located in monomer–monomer interfaces clustered close to the fragment C-terminus, predicted to contribute mainly to tetramer stability. Bottom panel: representation of the tetrameric fragment surface, colored according to calculated electrostatic properties. Red and blue colors indicate negatively and positively charged surface patches, respectively.

Modeling of the P protein oligomerization domain

The availability of the atomic structure of the Sendai virus P protein multimerization domain prompted us to compare the amino acid sequences of P proteins from different members of the *Paramyxoviridae* family, including HRSV P, searching for homology in that segment. P protein sequences from viruses indicated in Figure 7(A) were withdrawn from databases and aligned using the multiple sequence alignment algorithm ClustalW.[32] Interestingly, despite differences in protein length and the lack of overall homology, a short segment spanning residues Leu373 to Pro432 of the Sendai virus P protein—included in its tetramerization domain—, appeared to exhibit an appreciable degree of similarity with all paramyxovirus P proteins [Fig. 7(A), top]. Conservation values were more significant in a shorter subsection spanning residues Phe402 to Leu424 of the SeV P sequence, in which a repetitive pattern of hydrophobic amino acids resembled a short, but clear, heptad repeat. In the case of the HRSV P sequence,

these conserved residues were Ile131, Ile138, Leu146, Leu149, and Val153. Since the multiple sequence alignment indicated an evolutionary relationship between SeV and HRSV P proteins (as well as for the rest of the P sequences), at least in the segment shown in Figure 7(A), a 3D structure of the HRSV P protein segment could be modeled using homology-modeling methodologies.

Using the SeV P protein template, HRSV fragment X could be modeled as an elongated tetrameric coiled-coil. Residue conservation upstream of the heptad repeat-like segment was not as high as desirable for modeling purposes, and the initial ClustalW based alignment did not offer enough confidence to ensure high quality modeling. To overcome this difficulty and to extend the model of the multimerization domain up to residue Leu373 of the SeV P protein sequence, a direct alignment, without gaps, was generated, and a 3D model was obtained for the corresponding HRSV P protein segment, using the methodology indicated under Materials and Methods. This first approach did not result in a feasible model,

since the tetramer based on this alignment, although consistent in the region covered by the heptad repeats, presented structural inconsistencies near the N-terminal boundary. For instance, a group of glutamic acid side chains (residues Glu113, Glu114, and Glu115) pointed to each other in the inner side of the tetramer (not shown). Based on this first low quality model and using values of structural stability as an indicator (applying the GRO-MOS 43B1 force field implemented in the program Deep View), several alternate models were generated by introducing a single or a double gap in different positions of the alignment between SeV and HRSV P protein multi-merization domains. For each one of these alignments, a structural model was generated and examined, searching for spatial incompatibilities or atom clashes between amino acids of the four α-helices. Using this methodology and searching for energy-minimized feasible structures, the model shown in Figure 7(A) (bottom) was obtained, which corresponds to the structure-based alignment shown in Figure 7(A) (top).

The tetrameric model of HRSV P fragment X includes a bundle of four coiled-coil parallel α-helices with a two-residue gap between Tyr120 and Glu121. Thus, the α-helix of each monomer is interrupted by a nonstructured short section from Tyr120 to Glu122. Stability of the tetramer is maintained by a cluster of hydrophobic residues near the C-terminal end (Ile131, Leu135, Ile138, Leu142, Ile145, Leu146, Leu149, Leu152, and Val153) and by four Phe109 (one from each monomer) in the region close to the N-terminal end [green spheres in Fig. 7(B), top]. Some other electrostatic contacts appear to help to stabilize the complex as, for instance, the interaction between pairs Asp136/Arg134 or Glu140/Lys141 from adjacent monomers.

The location of the nonstructured loop in the vicinity of Ser119 offers an explanation for the generation of the two protease-resistant fragments, X and Y* (mentioned earlier). This loop, although short, appears to have a higher motility than the surrounding areas that contain structured α helices, and so it may be a clear target for chymotrypsin to generate the 42 amino acids long fragment Y*.

Interestingly, when a surface electrostatic map of the model is represented [Fig. 7(B), bottom], a clear asymmetry appears in charge distribution. The N-proximal end exhibits net electronegative properties, because of the external location of the side chain of glutamic acids 104, 107, 113, 114, 115, and Asp110 present in this area and to the lack of positively charged residues in the surrounding area. In contrast, the central part of the molecule shows an alternate nature of positively and negatively charged amino acids, equilibrating one to each other and resulting in absence of a net charge. The C-terminal end is characterized by the presence of large number of hydrophobic residues, contributing to the tetramer structural stability.

DISCUSSION

The solution molecular masses of the HRSV P protein and its trypsin-resistant fragment X have been determined by sedimentation equilibrium. The data demonstrate that both molecules are tetrameric in the range of protein concentrations used in our sedimentation studies, settling a long-standing controversy about the oligomeric status of HRSV P. The fact that P and fragment X elute from gel filtration columns with apparent molecular weights much higher than those expected for homotetramers[21] (~500 kDa for P protein and ~120 kDa for fragment X) is likely a consequence of their elongated structures. Indeed, the hydrodynamic parameters determined by sedimentation velocity analysis, especially the f/f_0 frictional ratio, indicated that both molecules, and particularly the full-length P protein, have very elongated shapes. This is in agreement with the thin rod-like structures of P protein molecules observed by electron microscopy. The length of these molecules (~12.5 nm) is slightly shorter than the C-terminal half of the Sendai virus P protein (named the PCT domain) that has been estimated to be 16-nm long. This PCT domain includes the P protein oligomerization domain (that overlaps with the polymerase binding site) and the site for binding to the N-RNA template.[9] It is worth stressing that Sendai virus P is 568 amino acids long and that its PCT domain spans the C-terminal 248 amino acids, which is similar in length to the entire HRSV P protein (241 amino acids).

The P protein gene of viruses of the *Paramyxovirinae* subfamily (including Sendai virus) encodes a plethora of polypeptides by means of pseudotemplated addition of nucleotides, known as RNA editing.[38] Because of this mechanism, sequences of the N-terminal half of the P protein are also represented in other gene products that, in general, are involved in counteracting the host interferon response. In HRSV, inhibition of the interferon response is mediated by extra genes (e.g., NS1 and NS2) that are not present in viruses of the *Paramyxovirinae* subfamily.[39] Thus, it is conceivable that HRSV P has maintained throughout evolution the minimal requirements necessary to act as a cofactor of the RNA-dependent RNA polymerase, but has lost (or has not gained) other accessory activities that, in this virus, are carried out by separate gene products. This explains the small size of HRSV P and the structural resemblance with only the PCT domain of the larger Sendai virus P protein. Since there are also structural similarities between the PCT domains of viruses of the *Paramyxovirinae* subfamily,[40] the resemblance of HRSV P with PCTs can be probably extended to the phosphoproteins of all viruses of the *Paramyxoviridae* family.

The thermal denaturation/renaturation curves observed for the HRSV P protein [Fig. 4(A)] likely result from the sum of temperature dependant changes in unstructured

parts of the molecule combined with melting of multiple structural motifs in more ordered parts of the protein. Furthermore, it is apparent that these motifs have different melting temperatures and that they are only partially renatured after a single cycle of heating and cooling. In a previous study, bioinformatical analysis of the P protein primary structure predicted the existence of two intrinsically disordered regions flanking a central structural domain that included fragment X.[21] Those disordered regions, in which some short α-helices were also predicted [Fig. 1(A)], may account for the gradual loss of CD intensity of P protein at $MRE_{222 \, nm}$ observed after stepwise heating of the protein sample.

The thermostability analysis of fragment X yielded results significantly different from those of the full-length protein. In this case, the melting curve is biphasic, consisting of a gradual reduction in the intensity of the $MRE_{222 \, nm}$ between 20 and 75°C and an accompanying steep reduction in CD above 75°C. First, these results demonstrate that, on a residue basis, fragment X contains much more ordered structure than full-length P protein. Moreover, the two phases in the melting curve likely result from (i) largely uncooperative temperature dependant changes in the far UV CD spectrum of less-ordered parts of the molecule (most apparent between 20 and 75°C) and (ii) a strongly cooperative high temperature transition (75–95°C) of a more ordered α-helical structure. The melting curve of fragment Y* demonstrates that this fragment contains slightly more α-helical structure on a residue basis than X. Moreover, the high temperature transition is even more pronounced, revealing that Y* is a homogeneous and highly thermostable structural motif contained within X. Notably, fragment Y* showed an almost complete gain of α-helical content after a single cycle of heating and cooling. Based on these data, it is likely that fragment Y* forms a compact four helical bundle and that this represents the minimal element of the oligomerization domain in the HRSV P protein.

The thermostability results obtained with fragments X and Y* are in good agreement with the model presented in Figure 7, even though the modeling exercise was carried out independent of the thermostability experiments. In the structural model of fragment X, the α-helices of each monomer that form the homotetrameric coiled-coil are interrupted by a two amino acid nonhelical spacer. The location of this spacer coincides closely with the N-terminal domain of fragment Y*, consistent with the generation of this fragment by limited digestion of fragment X with chymotrypsin. It is thus possible that some of the biphasic nature of the melting profile observed for fragment X is due to denaturation of the short N-terminal α-helices in the lower temperature part of the profile and that the high temperature transition results from the unfolding of the longer C-terminal four-helical bundle only. Based on the reversible denaturation and renaturation observed with fragment Y*, it is possible that only the C-terminal four-helical bundle of fragment X is able to fully renature after cooling. This idea is supported by the fact that the far UV CD spectrum of fragment X is only partially recovered when the sample was cooled below 70°C, whereas the α-helical content of the CD spectrum of fragment Y* is almost entirely recovered upon lowering the temperature from 95 to 20°C. These data are consistent with the presence of a hydrophobic core only in fragment Y*, which may direct the rapid renaturation of the four-helix bundle upon cooling.

The model presented in Figure 7 is also supported by other structural data provided in this study. For instance, the analytical ultracentrifugation studies demonstrate that fragment X is an elongated tetrameric molecule, and the CD studies reveal that it has a high α-helical content. Furthermore, as an additional test of the model, the sedimentation coefficient was calculated from the atomic coordinates of the model using the hydrodynamic modeling program HYDROPRO.[41] Using this procedure a value of $S_{20,w} = 2.3$ was obtained, in good agreement with the experimental value (2.21 ± 0.01) obtained by sedimentation velocity (Table I).

It is worth noting the asymmetric distribution of certain residues in fragment X, particularly the basic and hydrophobic amino acids that are concentrated in the C-terminal half of this fragment. It is tempting to speculate that this asymmetric amino acid distribution reflects the interaction of this part of the HRSV P protein with other components of viral or cellular origin. Notably, the site of interaction of the viral polymerase with the P protein of the bovine RSV has been mapped between amino acids 121 and 160,[16] included in fragment Y*.

In summary, the results reported here provide new insights into the structure of the HRSV P protein, particularly its tetrameric stoichiometry and the structural properties of its oligomerization domain. Moreover, the small size of this molecule, compared with the orthologues in other paramyxoviruses, makes it an attractive candidate for structural studies of this type of cofactor of paramyxoviral polymerases. The model we have derived for the oligomerization domain of HSRV P is in good agreement with experimental data and provides the structural basis for a rational approach to test the significance of individual amino acids in structural/functional studies of the HRSV and other paramyxoviral P proteins.

ACKNOWLEDGMENTS

Informatics SL-www.biomol-informatics.com" for bioinformatic consulting.

REFERENCES

1. Collins PL, Hill MG, Camargo E, Grosfeld H, Chanock RM, Murphy BR. Production of infectious human respiratory from cloned cDNA confirms an essential role for the transcription elongation factor from the 5′ proximal open reading frame of the M2 mRNA in gene expression and provides a capability for vaccine development. Proc Natl Acad Sci USA 1995;92:11563–11567.

2. Collins PL, Chanock RM, Murphy BR. Respiratory syncytial virus. In: Knipe DM, Howley PM, Griffin DE, Lamb RA, Martin MA, Roizman B, Straus SE, editors. Fields virology, 4th ed. Philadelphia: Lippincott Williams and Wilkins; 2001. pp 1443–1485.

3. Melero JA. Molecular biology of human respiratory syncytial virus. In: Cane PA, editor. Perspectives in medical virology, Vol. 14: Respiratory syncytial virus. Amsterdam: Elsevier; 2007. pp 1–42.

4. Stec DS, Hill MG, Collins PL. Sequence analysis of the polymerase L gene of human respiratory syncytial virus and predicted phylogeny of nonsegmented negative-strand virus. Virology 1991;183:273–287.

5. Collins PL, Hill MG, Cristina J, Grosfeld H. Transcription elongation factor of respiratory syncytial virus, a nonsegmented negative-strand RNA virus. Proc Natl Acad Sci USA 1996;93:81–85.

6. Huang YT, Collins PL, Wertz GW. Characterisation of the 10 proteins of human respiratory syncytial virus: identification of a fourth envelope-associated protein. Virus Res 1985;2:157–173.

7. Curran J, Marq JB, Kolakofsky D. An N-terminal domain of the Sendai paramyxovirus P protein acts as a chaperone for the NP protein during the nascent chain assembly step of genome replication. J Virol 1995;69:849–855.

8. Mavrakis M, Méhouas S, Réal R, Iseni F, Blondel D, Tordo N, Ruigrok RWH. Rabies virus chaperone: identification of the phosphoprotein peptide that keeps nucleoprotein soluble and free from non-specific RNA. Virology 2006;349:422–429.

9. Blanchard L, Tarbouriech N, Blackledge M, Timmins P, Burmeister WP, Ruigrok RWH, Marion D. Structure and dynamics of the nucleocapsid-binding domain of the Sendai virus phosphoprotein in solution. Virology 2004;319:201–211.

10. Curran J. A role for the Sendai virus P protein trimer in RNA synthesis. J Virol 1998;72:4274–4280.

11. Johansson K, Bourhis JM, Campanacci V, Cambillau C, Canard B, Longhi S. Crystal structure of the measles virus phosphoprotein domain responsible for the induced folding of the C-terminal domain of the nucleoprotein. J Biol Chem 2003;278:44567–44573.

12. Kingston RL, Hamel DJ, Gay LS, Dahlquist FW, Matthews BW. 2004. Structural basis for the attachment of a paramyxoviral polymerase to its template. Proc Natl Acad Sci USA 2004;101:8301–8306.

13. García-Barreno B, Delgado T, Melero JA. Identification of protein regions involved in the interaction of human respiratory syncytial virus phosphoprotein and nucleoprotein: significance for nucleocapsid assembly and formation of cytoplasmic inclusions. J Virol 1996;70:801–808.

14. Castagné N, Barbier A, Bernard J, Rezaei H, J-C, Huet J-C, Henry C, Da Costa B, Eléouët J-F. Biochemical characterization of the respiratory syncytial virus P-P and P-N protein complexes and localization of the P protein oligomerization domain. J Gen Virol 2004; 85:1643–1653.

15. Tran T-L, Castagné N, Bhella D, Varela PF, Bernard J, Chilmonczyk S, Berkenkamp S, Benhamo V, Grznarova K, Grosclaude J, Nespoulos C, Rey FA, Eléouët J-F. The nine C-terminal amino acids of the respiratory syncytial virus P are necessary and sufficient for binding

16. to ribonucleoprotein complexes in which six ribonucleotides are contacted per N protein protomer. J Gen Virol 2007;88:196–206.

16. Khattar SK, Yunus AS, Samal SK. Mapping the domains on the phosphoprotein of bovine respiratory syncytial virus required for N-P and P-L interactions using a minigenome system. J Gen Virol 2001;82:775–779.

17. Mason SW, Aberg E, Lawetz C, DeLong R, Whitehead P, Liuzzi M. Interaction between human respiratory syncytial virus (RSV) M2-1 and P proteins is required for reconstitution of M2-1 dependent RSV minigenome activity. J Virol 2003;77:10670–10676.

18. Tarbouriech N, Curran J, Ruigrok RWH, Burmeister WP. Tetrameric coiled coil domain of Sendai virus phosphoprotein. Nat Struct Biol 2000;7:777–781.

19. Rahaman A, Srinivasan N, Shamala N, Shaila MS. Phosphoprotein of the rinderpest virus forms a tetramer through a coiled coil region important for biological function. J Biol Chem 2004;279: 23606–23614.

20. Asenjo A, Villanueva N. Regulated but not constitutive human respiratory syncytial virus (HRSV) P protein phosphorylation is essential for oligomerization. FEBS Lett 2000;467:279–284.

21. Llorente MT, García-Barreno B, Calero M, Camafeita E, López JA, Longhi S, Ferrón F, Varela PF, Melero JA. Structural analysis of the human respiratory syncytial virus phosphoprotein: characterization of an α-helical domain involved in oligomerization. J Gen Virol 2006;87:159–169.

22. Hengst U, Kiefer P. Domains of human respiratory syncytial virus P protein essential for homodimerization and for binding to N and NS1 protein. Virus Genes 2000;20:221–225.

23. Tarbouriech N, Curran J, Ebel C, Ruigrok RWH, Burmeister WP. On the domain structure and the polymerization state of the Sendai virus P protein. Virology 2000;266:99–109.

24. García J, García-Barreno B, Martinez I, Melero JA. Mapping of monoclonal antibody epitopes of the human respiratory syncytial virus P protein. Virology 1993;195:239–242.

25. Laue TM, Shah BD, Ridgeway TM, Pelletier SL. Computer-aided interpretation of analytical sedimentation data for proteins. In: Harding SE, Rowe AJ, Horton JC, editors. Analytical ultracentrifugation in biochemistry and polymer science. Cambridge, United Kingdom: The Royal Society of Chemistry; 1992. pp 90–125.

26. Schuck P, Perugini MA, Gonzales NR, Howlett GJ, Schubert D. Size-distribution analysis of proteins by analytical ultracentrifugation: strategies and application to model systems. Biophys J 2002;82:1096–1111.

27. Vistica J, Dam J, Balbo A, Yikilmaz E, Mariuzza RA, Rouault TA, Schuck P. Sedimentation equilibrium analysis of protein interactions with global implicit mass conservation constraints and systematic noise decomposition. Anal Biochem 2004;326:234–256.

28. Schuck P. Size-distribution analysis of macromolecules by sedimentation velocity ultracentrifugation and Lamm equation modelling. Biophys J 2000;78:1606–1619.

29. Wrigley NG, Brown EB, Skehel JJ. Electron microscopy of influenza virus. In: Harris JR, Horne RW, editors. Electron microscopy of proteins, Vol. 5: Viral structure. London: Academic Press; 1986. pp. 103–163.

30. Morris MC, Mery J, Heitz A, Heitz F, Divita G. Design and synthesis of a peptide derived from positions195-244 of human cdc25C phosphatase. J Pept Sci 1999;5:263–271.

31. Altschul SF, Gish W, Miller W, Myers EW, Lipman DJ. Basic local alignment search tool. J Mol Biol 1990;215:403–410.

32. Thompson J D, Higgins DG, Gibson TJ. CLUSTAL W: improving the sensitivity of progressive multiple sequence alignment through sequence weighting, position-specific gap penalties and weight matrix choice. Nucleic Acids Res 1994;22:4673–4680.

33. Guex N, Peitsch MC. SWISS-MODEL and the Swiss-PdbViewer: an environment for comparative protein modeling. Electrophoresis 1997;18:2714–2723.

34. Peitsch MC. ProMod and Swiss-Model: internet-based tools for automated comparative protein modelling. Biochem Soc Trans 1996;24:274–279.

35. Schwede T, Kopp J, Guex N, Peitsch MC. SWISS-MODEL: an automated protein homology-modelling server. Nucleic Acids Res 2003; 31:3381–3385.

36. Hooft RW, Vriend G, Sander C, Abola EE. Errors in protein structures. Nature 1996;381:272.

37. Vriend G. WHAT IF: a molecular modelling and drug design program. J Mol Graph 1990;8:52–56.

38. Lamb RA, Kolakofsky D. *Paramyxoviridae*: The viruses and their replication. In: Knipe DM, Howley PM, Griffin DE, Lamb RA, Martin MA, Roizman B, Straus SE, editors. Fields virology, 4th ed. Philadelphia: Lippincott Williams and Wilkins; 2001. pp 1305–1340.

39. Conzelmann K-K. Transcriptional activation of α/β interferon genes: interference by nonsegmented negative-strand RNA viruses. J Virol 2005;79:5241–5248.

40. Karlin D, Ferron F, Canard B, Longhi S. Structural disorder and modular organization of *Paramyxovinae* N and P. J Gen Virol 2003; 84:3239–3252.

41. García de la Torre J, Huertas ML, Carrasco B. Calculation of hydrodynamic properties of globular proteins from their atomic-level structure. Biophys J 2000;78:719–730.